EurJIC
European Journal
of Inorganic Chemistry

ChemPubSoc
Europe

FULL PAPER

4,4′,5,5′-Tetrakis(guanidinyl)binaphthyl – Synthesis and Properties of Two Redox-Active Ligands and Oxidative C–C Coupling to Perylene Derivatives

Sven Wiesner,[a] Alexandra Ziesak,[a] Matthias Reinmuth,[a] Petra Walter,[a] Elisabeth Kaifer,[a] Hubert Wadepohl,[a] and Hans-Jörg Himmel*[a]

We report the synthesis and properties of the new redox-active ligands 4,4′,5,5′-tetrakis(tetramethylguanidinyl)binaphthyl and 4,4′,5,5′-tetrakis(N,N′-dimethylethyleneguanidinyl)binaphthyl. The first dinuclear zinc complexes were prepared. Oxidative C–C coupling of these compounds leads to perylene derivatives.

Introduction

Guanidines and guanidinates are well established as versatile ligands.[1–6] Hence, zinc guanidine–pyridine and guanidine–quinoline hybrid complexes have been shown to catalyse lactide polymerisation.[7] Copper(I) complexes of tripodal tris(2-guanidinylethyl)amine ligands react with dioxygen to yield end-on superoxido complexes, which represent models for the first step in the biological dioxygen reduction cascade and exhibit a rich chemistry.[8] The recent discovery of a halide-induced copper(I) disulfide/copper(II) thiolate conversion of a dinuclear copper complex with guanidinyl-functionalized disulfide ligands also adds to the interest in guanidine ligands.[9] Using experimental charge density studies, it was possible to directly prove the σ- and π-contributions to the metal–guanidine bond,[10] which express themselves by a significant elongation of the imino N=C bond length upon coordination. Recently, guanidinyl-functionalized aromatic compounds (GFAs) such as 1,2,4,5-tetrakis(tetramethylguanidinyl)benzene (**1**)[11] and 1,4,5,8-tetrakis(tetramethylguanidinyl)naphthalene (**2**, Scheme 1)[12] were introduced as a new class of strong organic electron donors and redox-active ligands. The electronic properties can be fine-tuned by modification of the guanidinyl groups[13] and/or substitution of the ring protons.[14] A number of late transition metal complexes of ligands **1** and **2** have already been synthesized and their redox chemistry studied.[12,15–17] An almost complete electron-transfer series was realized in the case of dinuclear copper complexes of ligand **1**. Hence, examples of complexes of the general type [Cu^I|**1**|Cu^I], [Cu^II|**1**|Cu^II], [Cu^I|**1**^2+|Cu^I] (in the form of a one-dimensional, semiconducting coordination polymer), [Cu^II|**1**^+|Cu^II] [featuring a high-spin (quartet) electronic ground state and strong metal–ligand ferromagnetic coupling] and [Cu^II|**1**^2+|Cu^II] have already been synthesized and completely characterized.[15]
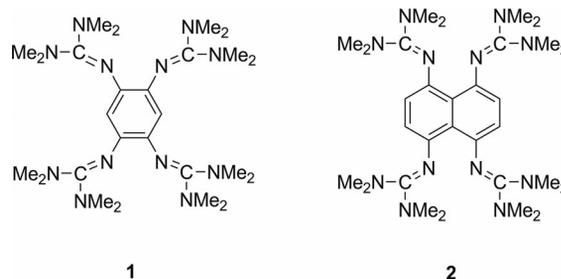
Scheme 1. Two known guanidine electron donors.

Herein we describe the synthesis and properties of the two new redox-active ligands 4,4′,5,5′-tetrakis(tetramethylguanidinyl)binaphthyl (**3a**) and 4,4′,5,5′-tetrakis(N,N′-di-

[a] Anorganisch-Chemisches Institut, Ruprecht-Karls-Universität Heidelberg,
Im Neuenheimer Feld 270, 69120 Heidelberg, Germany
Fax: +49-6221-545707
E-mail: hans-jorg.himmel@aci.uni-heidelberg.de
Homepage: http://www.uni-heidelberg.de/fakultaeten/chemgeo/aci/himmel/
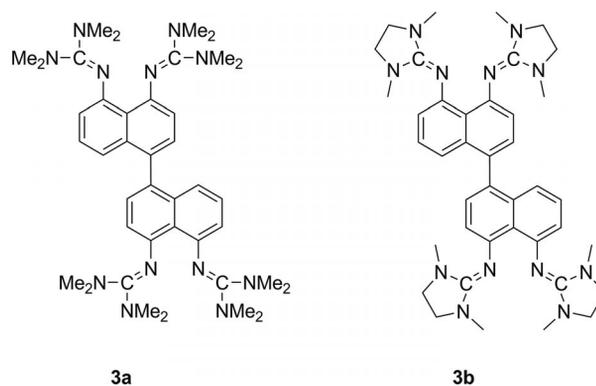
Scheme 2. Two new redox-active guanidine ligands **3a** and **3b**.

methylethyleneguanidinyl)binaphthyl (**3b**) sketched in Scheme 2. The two compounds represent proton sponges, like the two known compounds **2**[12] and 1,8-bis(tetramethylguanidinyl)naphthalene.[18,19] The synthesis of the first Zn complexes of **3a** and **3b** demonstrate their possible application as redox-active ligands. Oxidation leads to new tetraguanidinyl–perylene derivatives by oxidative C–C coupling.

Results and Discussion

Synthesis and Characterisation of 3a and 3b

Compounds **3a** and **3b** were synthesized starting from binaphthyl as shown in Scheme 3 for **3a**. Contrary to previous reports,[20] the nitration of binaphthyl with nitronium tetrafluoroborate in sulfolane only afforded 4,4′-dinitrobinaphthyl, not 4,4′,5,5′-tetranitrobinaphthyl. Instead, the reaction of binaphthyl with nitric acid and sulfuric acid in glacial acetic acid led to the desired first product 4,4′,5,5′-tetranitrobinaphthyl.[20] The two substituted binaphthyls 4,4′-dinitrobinaphthyl and 4,4′,5,5′-tetranitrobinaphthyl were purified by crystallization. Their molecular structures as derived from X-ray diffraction are displayed in Figure 1. The dihedral angle between the two naphthyl planes is 60.6° in the dinitro and 87.0° in the tetranitro compound. The nitro groups of the tetrasubstituted binaphthyl in the 4- and 5-positions and those in 4′- and 5′-positions are oriented parallel to each other, with N···N separations of 288.8 and 290.1 pm. The reduction of 4,4′,5,5′-tetranitrobinaphthyl with hydrazine monohydrate and palladium on activated
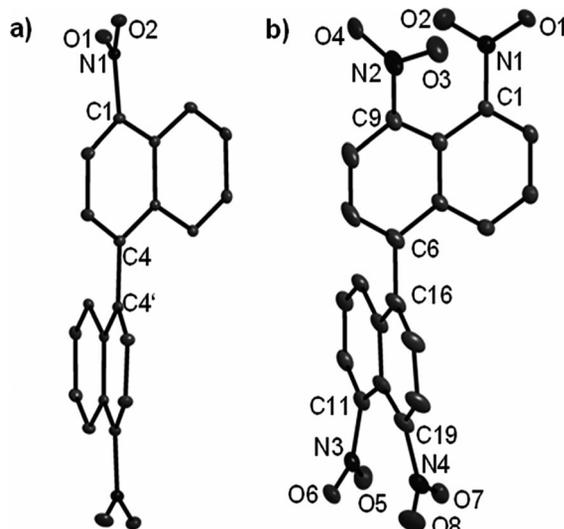
Figure 1. Molecular structures of (a) 4,4′-dinitrobinaphthyl and (b) 4,4′,5,5′-tetranitrobinaphthyl. Vibrational ellipsoids are drawn at the 50% probability level. Hydrogen atoms attached to carbon omitted for sake of clarity. Selected bond lengths [pm] and bond angles [°] for 4,4′-dinitrobinaphthyl: O1–N1 122.4(2), O2–N1 123.7(2), N1–C1 147.8(2), C1–C2 136.0(3), C1–C10 142.0(3), C2–C3 140.1(3), C3–C4 137.4(3), C4–C4′ 149.5(4), C4–C5 143.1(3), C5–C6 142.4(3), C6–C7 136.5(3), C7–C8 140.9(3), C8–C9 136.7(3), C9–C10 141.8(3); O1–N1–O2 123.58(17), C5–C4–C4′–C5′ –60.62(3). Selected bond lengths [pm] for 4,4′,5,5′-tetranitrobinaphthyl: N1–O1 119.3(5), N1–O2 125.7(5), N1–C1 146.0(5), N2–O3 127.5(6), N2–O4 124.5(11), N2–C9 146.0(6), N3–O5 122.7(4), N3–O6 122.6(4), N3–C11 146.4(5), N4–O7 122.8(5), N4–O8 123.1(5), N4–C19 147.4(6), C6–C16 149.3(6).
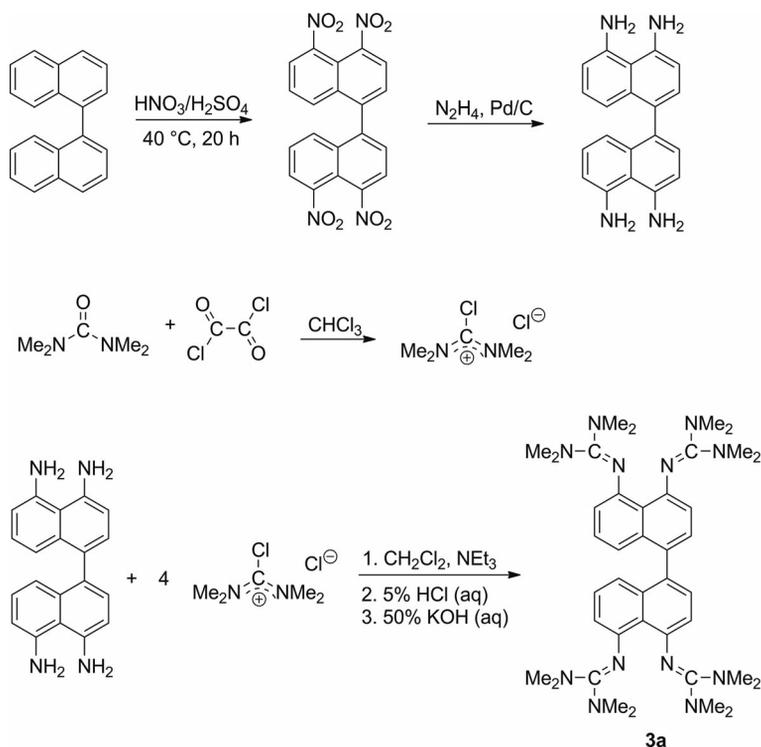
Scheme 3. Synthesis of **3a** from binaphthyl.

charcoal as catalyst afforded the second product on the way to the new guanidine ligands, 4,4′,5,5′-tetraaminobinaphthyl.

The targeted new ligand **3a** was then obtained by reaction of the Vilsmeier salt 2-chloro-1,1′,3,3′-tetramethylformamidinium chloride {[(Me$_2$N)$_2$CCl]Cl}, freshly prepared from tetramethylurea and oxalyl chloride, with 4,4′,5,5′-tetraaminobinaphthyl in the presence of the base NEt$_3$. It is soluble in most common organic solvents such as acetonitrile, dichloromethane or toluene. Compound **3b** could be synthesized in an analogous way with 2-chloro-1,3-dimethylimidazolium chloride in place of 2-chloro-1,1′,3,3′-tetramethylformamidinium chloride. Both ligands were characterized by NMR spectroscopy, mass spectrometry, elemental analysis and absorption spectroscopy in the UV/Vis region. The absorption spectra are very sensitive to changes in the electronic structure. It is shown in Figure 2 for **3a** dissolved in CH$_3$CN. The two intense bands centred at 220 and 237 nm fall into a region typical for binaphthyls. For comparison, 1,1′-binaphthyl exhibits an intense band at ca. 220 nm and a weaker band containing vibrational fine structure at ca. 290 nm.[21] For 2,2′-bis(tetramethylguanidinyl)-1,1′-binaphthyl, four bands appeared at 214, 255, 304 and 351 nm.[22] Of these, the first two were assigned to electronic transitions primarily involving the binaphthyl π-electrons. In addition, the spectra of **3a** and **3b** feature an

absorption at lower energies (λ = 360 nm), which can be assigned to an electronic transition involving the guanidinyl groups.

Dinuclear Zn Complexes

The reaction of **3a** or **3b** with 2 equiv. of ZnCl$_2$ yielded the dinuclear complexes [**3a**(ZnCl$_2$)$_2$] (Scheme 4) and [**3b**(ZnCl$_2$)$_2$]. Of these two complexes, [**3a**(ZnCl$_2$)$_2$] can be crystallized from CHCl$_3$ solutions, and its molecular structure is illustrated in Figure 3. As expected, the zinc atoms are κ^2-coordinated with Zn–N bond lengths of ca. 200 pm.
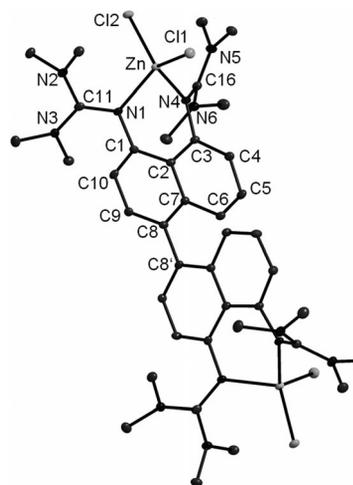
Figure 3. Molecular structure of [**3a**(ZnCl$_2$)$_2$]. Vibrational ellipsoids drawn at the 50% probability level. Hydrogen atoms attached to carbon omitted for clarity. Selected bond lengths [pm] and bond angles [°]: Zn–Cl1 225.90(10), Zn–Cl2 225.25(11), Zn–N1 200.2(3), Zn–N4 200.9(3), N1–C1 141.8(4), N1–C11 133.0(5), N2–C11 135.4(5), N3–C11 136.4(5), N4–C3 141.0(4), N4–C16 133.9(5), N5–C16 135.1(5), N6–C16 135.4(5), C1–C2 144.1(5), C1–C10 138.9(5), C2–C3 144.6(5), C2–C7 144.4(5), C3–C4 138.9(5), C4–C5 140.1(5), C5–C6 135.8(5), C6–C7 142.8(5), C7–C8 143.2(5), C8–C8′ 149.9(6), C8–C9 136.2(5), C9–C10 141.3(5); Cl1–Zn–Cl2 115.58(4), N1–Zn–N4 89.55(12); C7–C8–C8′–C7′ 75.33(2).

The dihedral angle between the two naphthyl planes is 75.4°. The Zn atoms are displaced from the naphthyl planes by 112 pm. As is typical for coordinated guanidines, the N=C bonds are relatively long [133.0(5) and 133.9(5) pm].[10]

Figure 2. UV/Vis spectra of **3a** and [**4a**H$_2$](PF$_6$)$_4$ in acetonitrile.
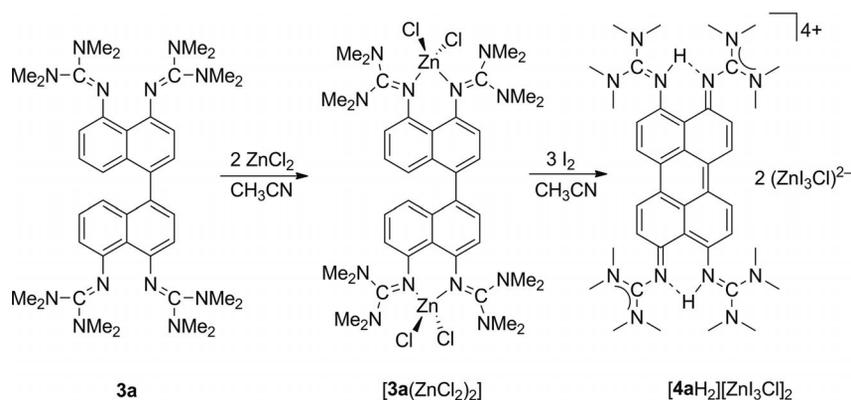
Scheme 4. Synthesis of the dinuclear complex [**3a**(ZnCl$_2$)$_2$] and its oxidation with I$_2$ in acetonitrile to [**4a**H$_2$][ZnI$_3$Cl]$_2$.

Oxidation Experiments

Chemical oxidation of the two compounds was performed with I_2 or $AgPF_6$ (Scheme 5). In both cases oxidative C–C coupling in the *peri* position of the aromatic system was observed. The two protons released in this process were captured by the guanidinyl groups. Hence, the products were the twofold oxidized and deprotonated perylene cations $[4aH_2]^{4+}$ and $[4bH_2]^{4+}$. The ^1H NMR spectrum of $[4aH_2](PF_6)_2$ in CD_3CN is shown in Figure 4a. The N–H protons gave rise to a sharp signal at $\delta = 12.46$ ppm. This position is characteristic for proton sponges with a (asymmetric) bridging N–H···N bonding situation. For comparison, the corresponding signals were reported at $\delta = 14.45$ and 14.28 ppm for **2** and 1,8-bis(tetramethylguanidinyl)-naphthyl, respectively. As a result of the C–C bond formation, only one singlet at $\delta = 3.17$ ppm for the methyl protons can be observed. The UV/Vis spectrum of the salt $[4aH_2](PF_6)_4$ (Figure 2) is clearly different to that of **3a**.
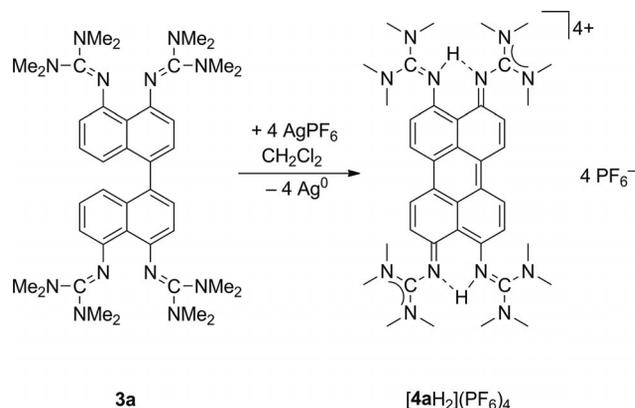
Scheme 5. Oxidative C–C coupling of **3a** with $AgPF_6$ to the perylene derivative $[4aH_2](PF_6)_4$ in dichloromethane.
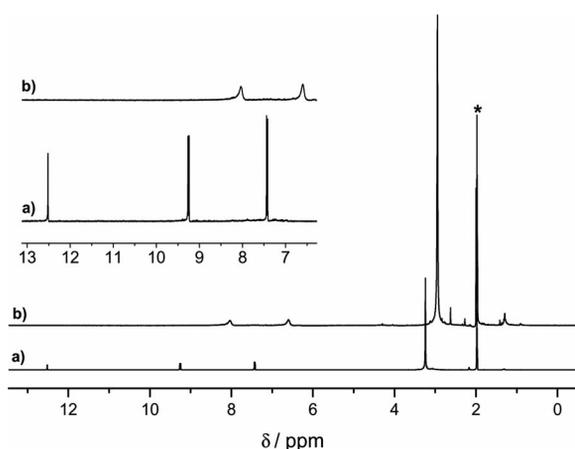
Figure 4. ^1H NMR spectra (200 MHz, CD_3CN) of (a) $[4aH_2]$-$(PF_6)_4$ and (b) **4a**. The labelled signal (*) stems from solvent.

It contains a relatively broad and intense absorption band centred at 500 nm that shows a strong but not clearly resolved vibrational progression, typical for a $\pi^* \leftarrow \pi$ transition in polycondensed aromatics and especially in perylene derivatives.[23] The twofold oxidized and protonated per-

ylene derivative could be crystallized in the form of the salt $[4aH_2](PF_6)_4$. Figure 5 displays its structure as derived from the XRD analysis. The N–H protons are statistically distributed with equal probability on both sites of the NHN bridges. Moreover, due to the statistical distribution of the N–H protons (Figure 5), the analysis of the XRD data returns averaged bond lengths. Therefore, all four N–H hydrogen positions in Figure 5 are occupied by half of an atom. The shortening of the C1–C2 bond to 134.6(7) ppm in contrast to all other C–C bonds within the ring system indicates destruction of the aromatic character. The C–N bond lengths from the C atoms in the oxidized perylene ring to the four guanidinyl substituents are all equally long [135.2(7) ppm]. This can be explained by several mesomeric formulas (Scheme 5 shows one of them). Quantum chemical calculations (BP86/SVP) predict the stretching mode ν(N–H) to occur at 3068 cm^{-1}, in the same region as the ν(C–H) modes. Therefore, an unambiguous assignment of the ν(N–H) mode in the IR spectra was not possible {see the IR spectra of $[4aH_2](PF_6)_2$ and $[4bH_2](PF_6)_2$ in the Supporting Information}.
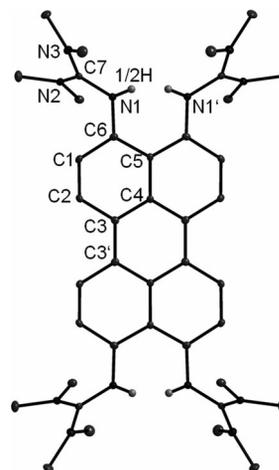
Figure 5. Illustration of the structure of the tetracation in the salt $[4aH_2](PF_6)_4$. Vibrational ellipsoids drawn at the 50% probability level. Hydrogen atoms attached to carbon and the anions are omitted for clarity. Please note that the N–H hydrogen positions are each occupied by half of an atom. Selected bond lengths [pm] and bond angles [°] with the corresponding values for $[4aH_2][ZnI_3Cl]_2$ given in brackets: N1–C6 135.2(7) [133.7(9)/138.2(9)], N1–C7 138.7(6) [136.5(10)/138.0(10)], N2–C7 131.8(7) [131.9(10)/132.3(11)], N3–C7 132.7(7) [132.3(12)/134.2(10)], C1–C2 134.6(7) [134.6(10)/137.4(10)], C1–C6 142.5(7) [144.4(10)/140.4(11)], C2–C3 143.7(7) [142.7(10)/141.9(10)], C3–C3′ 142.7(10) [142.5(9)], C3–C4 141.4(6) [143.1(10)/141.6(10)], C4–C5 143.8(10) [143.5(10)], C5–C6 143.5(6) [143.4(11)/141.5(10)]; C6–N1–C7 122.6(4) [120.8(6)/125.3(7)], N2–C7–N3 123.2(4) [121.7(7)/124.6(8)].

We also probed the redox activity of $[3a(ZnCl_2)_2]$ by reaction with an excess of I_2 (Scheme 4). NMR experiments indicated quantitative reaction to a single guanidine species. A small amount of dark green crystals precipitated from the solution. The analysis showed it to be the salt $[4aH_2][ZnI_3Cl]_2$ (see Scheme 4 and Supporting Information for an illustration of the structure; further halide exchange in the anion leads to a different average iodine/chlorine ra-

tio). This salt is an intermediate; reaction with further I_2 molecules leads finally to a salt of the composition $[4aH_2](I_3)_3I \cdot 2ZnCl_2$. Some bond parameters of $[4aH_2][ZnI_3Cl]_2$ and $[4aH_2](PF_6)_4$ are compared in the caption to Figure 5. Hence, the zinc–guanidine bonds were cleaved allowing for protonation of the guanidinyl groups to occur in the course of C–C coupling. Subsequently, we studied the redox properties in cyclovoltammetric (CV) experiments. Figure 6 shows the CV curves recorded for **3b** in dichloromethane with $[nBu_4N][PF_6]$ as supporting electrolyte at a scan rate of $100\,mV\,s^{-1}$ (CV curves for **3a** at different scan rates can be found in the Supporting Information). The curve form was reproduced several times. An explanation for all waves is not yet possible, and the following discussion is restricted to the most prominent features. The measurements show the existence of a two-electron oxidation wave at $E_{ox} = -0.27$ V vs. Fc/Fc$^+$. A further oxidation wave appears at higher potentials (double maximum at $E_{ox} = 0.42/0.52$ V vs. Fc/Fc$^+$). The total oxidation process is clearly not fully reversible (in line with the chemical oxidation results). In comparison to the oxidation waves, the reduction peaks are lower in intensity and experience substantial shifts. Further measurements, in which the potential was not raised above 0.2 V vs. Fc/Fc$^+$ (see Supporting Information), indicate that the first (two-electron) oxidation wave is reversible. The corresponding reduction peak is located at $E_{red} = -0.47$ V. It could be tentatively assigned to oxidation/reduction without C–C coupling, leading in the oxidation direction to double-bond formation between the two C_{10} ring systems (see the scheme in the Supporting Information). The large difference between E_{ox} and E_{red} could be explained by the significant structural changes that accompany this process. C–C coupling might then be responsible for the oxidation wave at higher potentials, and the double-maximum structure of the oxidation corresponds to a reduction peak at $E_{red} = -0.21/-0.09$ V vs. Fc/Fc$^+$. The reduction peak is absent in experiments in which the potential was kept below 1.2 V (see Supporting Information). Again, massive structural changes could be responsible for the large difference between E_{ox} and E_{red}.

Reduction and Deprotonation to the Neutral Perylenes 4a and 4b

The reduction and twofold deprotonation of both $[4aH_2]^{4+}$ and $[4bH_2]^{4+}$ with hydrazine monohydrate led to the formation of the neutral compounds **4a** and **4b** (Scheme 6).
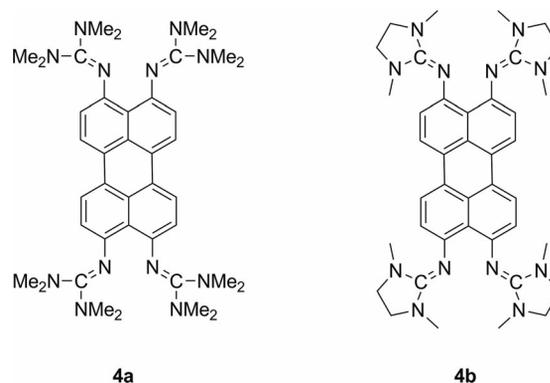
Scheme 6. Neutral 3,4,9,10-guanidinyl-substituted perylenes **4a** and **4b**.

In Figure 4 the ^{1}H NMR spectra of $[4aH_2]^{4+}$ and **4a** in CD$_3$CN are compared. After reaction with hydrazine, the two signals of the aromatic protons and the singlet for the methyl groups are shifted to higher field, which indicates restoration of the aromatic system. Additionally, the sharp signal of the two N–H protons at $\delta = 12.46$ ppm disappeared, which indicates deprotonation. Both **4a** and **4b** could also be identified by mass spectrometry. In the UV/Vis spectrum, the large absorption owing to the $\pi^* \leftarrow \pi$ transition shifts to lower energy and again displays a vibrational progression (maxima at 562, 525 and ca. 490 nm for **4a** and 549, 522 and ca. 487 nm for **4b**). The restoration of the aromatic perylene system is accompanied by the appearance of a strong fluorescence signal (ochre) that shows vibrational structure and with maximum intensity at 586 nm (with a shoulder at ca. 625 nm) for **4a** and 623 nm for **4b** (see Figure 7 and Supporting Information).[23] In contrast,

Figure 6. CV curve of **3b** in CH$_2$Cl$_2$ with $[nBu_4N][PF_6]$ as supporting electrolyte (Pt electrode, potential given relative to the Fc/Fc$^+$ redox couple, scan rate of $100\,mV\,s^{-1}$).
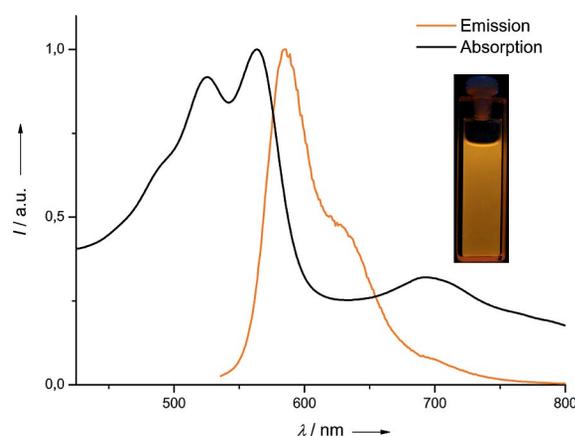
Figure 7. UV/Vis spectrum of **4a** (black) and its emission spectrum (orange) excited at $\lambda = 520$ nm (both spectra measured in dichloromethane) as well as a picture of the cuvette with the solution under UV light.

[**4a**H$_2$]$^{4+}$ and [**4b**H$_2$]$^{4+}$ are not fluorescent. Unfortunately, neither **4a** nor **4b** could be obtained free of salts, which hampered elemental analysis. Several attempts using other reducing agents, especially sodium in THF, in place of hydrazine monohydrate, were of limited success [although first small-scale (NMR) experiments looked promising]. In further experiments, a solution of the crude product **4a** in dichloromethane was protonated by using hydrochloric acid (10%). After addition, the aqueous phase turned brown-green and was separated from the almost colourless organic phase. The solution of the protonated product in water exhibits a strong green fluorescence, which demonstrates the pH dependence of the fluorescence wavelength.

Conclusions

We report the three-step synthesis of the two new redox-active guanidine ligands 4,4′,5,5′-tetrakis(tetramethylguanidinyl)binaphthyl and 4,4′,5,5′-tetrakis(*N*,*N*′-dimethylethyleneguanidinyl)binaphthyl. Their ligand properties were probed by the synthesis of the first dinuclear zinc complexes. Oxidation of the ligands led to oxidized and twofold protonated perylene systems by C–C coupling. Reduction to the 3,4,9,10-guanidinyl-substituted perylenes was studied, and the changes in the electronic structure were monitored by absorption and emission spectroscopy.

Experimental Section

General: All reactions were carried out under an inert gas atmosphere using standard Schlenk techniques. All starting materials and reagents were obtained commercially and used as delivered: 1,1′-binaphthyl (Aldrich, 97%), tetramethylurea (Aldrich, 99%), 1,3-dimethyl-2-imidazoline (ABCR, 98%), oxalyl chloride (Aldrich, 98%), triethylamine (Aldrich, 99.5%), hydrazine monohydrate (Fluka) and AgPF$_6$ (ABCR, 99%). The Pd/C (10%) catalyst was a gift from Prof. G. Huttner. UV/Vis measurements were performed with a Cary 5000 spectrophotometer. Infrared spectra were recorded with a BIORAD Excalibur FTS 3000. NMR spectra were measured with a Bruker Avance III 600, Bruker Avance II 400 or Bruker Avance DPX AC200 spectrometer. Elemental analyses were performed at the Microanalytical Laboratory of the University of Heidelberg. EI mass spectra were obtained with a Finnigan MAT 8230 or JEOL JMS-700 instrument. An EG&G Princeton 273 apparatus was used for the CV measurements.

4,4′-Dinitrobinaphthyl: The starting compound 1,1′-binaphthyl (776.8 mg, 3.05 mmol) was placed in a flask, and nitronium tetrafluoroborate solution (25 mL, 0.5 M) in sulfolane (12.5 mmol) was added dropwise with vigorous stirring. The reaction mixture was then heated to 80 °C for 75 min. After cooling to room temperature, water (50 mL) was added. The solution was stirred for 15 h, and the precipitate was collected. The crude product was recrystallized twice from glacial acetic acid. Crystals of 4,4′-dinitrobinaphthyl suitable for XRD analysis were obtained from a glacial acetic acid solution. ^{1}H NMR (200.13 MHz, CD$_2$Cl$_2$): δ = 8.61 (d, *J* = 8.6 Hz, 2 H, CH$_{ar.}$), 8.32 (d, *J* = 7.8 Hz, 2 H, CH$_{ar.}$), 7.76 (m, 2 H, CH$_{ar.}$), 7.60 (d, *J* = 7.8 Hz, 2 H, CH$_{ar.}$), 7.43 (m, 4 H, CH$_{ar.}$) ppm. Crystal data for C$_{20}$H$_{12}$N$_2$O$_4$: M_r = 344.32, 0.30 × 0.20 × 0.20 mm, monoclinic, space group *C*2/*c*, *a* =

13.370(3), *b* = 6.8320(14), *c* = 17.054(3) Å, β = 100.79(3)°, *V* = 1530.2(5) Å^3, *Z* = 4, $d_{calcd.}$ = 1.495 Mg m^{-3}, Mo-K_α radiation (graphite-monochromated, λ = 0.71073 Å), *T* = 100 K, θ_{range} = 2.43–27.49°. Reflections measd. 3507, indep. 1762, R_{int} = 0.0242. Final *R* indices [*I* > 2σ(*I*)]: R_1 = 0.0686, wR_2 = 0.1687.

4,4′,5,5′-Tetranitrobinaphthyl: To a suspension of 1,1′-binaphthyl (5.00 g, 19.66 mmol) in glacial acetic acid (70 mL) was added a cooled solution of fuming nitric acid (14.5 mL) and concentrated sulfuric acid (24.0 mL). The reaction mixture was kept at 10 °C during the addition. The reaction mixture was then heated to 40 °C for 20 h. After cooling to room temperature, ice/water (200 mL) was added. The precipitate was collected by filtration, washed with water and then dissolved in CH$_2$Cl$_2$ (300 mL). The solution was dried with CaCl$_2$, and the solvent was removed under vacuum. Upon recrystallization from glacial acetic acid, the product precipitated as a light yellow solid (5.55 g, 12.8 mmol, 65%). ^{1}H NMR (600.13 MHz, [D$_8$]THF): δ = 8.55 (d, *J* = 7.7 Hz, 2 H), 8.39 (d, *J* = 7.5 Hz, 2 H), 7.93 (d, *J* = 7.7 Hz, 2 H), 7.79 (d, *J* = 8.5 Hz, 2 H), 7.68 (t, *J* = 8.0 Hz, 2 H) ppm. ^{13}C NMR (150.92 MHz, [D$_8$]THF): δ = 147.29, 147.24, 143.07, 135.37, 132.97 (CH), 129.99 (CH), 128.38 (CH), 127.89 (CH), 117.69 ppm. Crystal data for C$_{20}$H$_{10}$N$_4$O$_8$: M_r = 434.32, 0.30 × 0.30 × 0.30 mm, monoclinic, space group *C*2/*c*, *a* = 23.696(5), *b* = 8.9380(18), *c* = 17.312(4) Å, β = 97.86(3)°, *V* = 3632.1(13) Å^3, *Z* = 8, $d_{calcd.}$ = 1.588 Mg m^{-3}, Mo-K_α radiation (graphite-monochromated, λ = 0.71073 Å), *T* = 100 K, θ_{range} = 2.38–27.55°. Reflections measd. 33656, indep. 4194, R_{int} = 0.0841. Final *R* indices [*I* > 2σ(*I*)]: R_1 = 0.1124, wR_2 = 0.2889.

4,4′,5,5′-Tetraamino-1,1′-binaphthyl: A suspension of 4,4′,5,5′-tetranitrobinaphthyl (1.30 g, 2.99 mmol) and Pd/C (0.39 g, 10%) as catalyst in dry ethanol (30 mL) was heated to 50 °C, and hydrazine monohydrate (5.2 mL, 107 mmol) was slowly added. Subsequently, the reaction mixture was stirred at 85 °C for 2 h. After cooling to room temperature, the reaction mixture was filtered through silica to afford a deep purple solution. The solvent was removed under vacuum. The solid was washed with water to remove excess hydrazine monohydrate, and the green solid was dried under vacuum (0.630 g, 2.01 mmol, 67%). ^{1}H NMR (399.89 MHz, [D$_8$]THF): δ = 7.14 (m, 2 H, CH$_{ar.}$), 6.95 (m, 2 H, CH$_{ar.}$), 6.79–6.75 (m, 2 H, CH$_{ar.}$), 6.63–6.59 (m, 2 H, CH$_{ar.}$), 6.49–6.47 (m, 2 H, CH$_{ar.}$), 5.09 (br. s, 8 H, NH) ppm.

4,4′,5,5′-Tetrakis(tetramethylguanidinyl)binaphthyl (3a): To a solution of *N*,*N*,*N*′,*N*′-tetramethylurea (0.84 mL, 6.88 mmol) dissolved in dry CHCl$_3$ (20 mL) was added oxalyl chloride (2.96 mL, 34.4 mmol) dropwise. The yellow solution was stirred at reflux for 16 h. The solvent was removed under vacuum. The remaining solid, 2-chloro-1,1′,3,3′-tetramethylformamidinium chloride (6.88 mmol), was washed twice with Et$_2$O (5 mL), dissolved in dry CH$_2$Cl$_2$ (10 mL) and then added dropwise to a dry CH$_2$Cl$_2$ solution (25 mL) containing 4,4′,5,5′-tetraaminobinaphthyl (0.45 g, 1.43 mmol) and triethylamine (2.35 mL, 17.16 mmol) at –10 °C. The reaction mixture was stirred for an additional period of 3 h and warmed up to room temperature during this time. The solution was extracted with HCl (5%) and then deprotonated with KOH solution (50%). After extraction with CH$_2$Cl$_2$, the combined organic phases were dried with K$_2$CO$_3$, and the solvent was removed under vacuum. The solid was extracted with hexane, filtered, and the solvent was removed under vacuum to afford the crude product as a red-orange solid (0.637 g, 0.95 mmol, 63%). C$_{40}$H$_{58}$N$_{12}$ (706.49): calcd. C 67.96, H 8.27, N 23.76; found C 67.71, H 8.07, N 23.84. ^{1}H NMR (399.89 MHz, CD$_2$Cl$_2$): δ = 7.13 (d, 2 H, CH$_{ar.}$), 6.94 (t, 2 H, CH$_{ar.}$), 6.76 (d, 2 H, CH$_{ar.}$), 6.34 (d, 2 H, CH$_{ar.}$), 6.21 (d, 2 H, CH$_{ar.}$), 2.74 [s, 24 H, N(CH$_3$)$_2$], 2.71 [s, 24 H, N(CH$_3$)$_2$]

ppm. $^{13}C\{^1H\}$ NMR (100.55 MHz, CD_2Cl_2): δ = 155.09 (C=N), 154.92 (C=N), 150.71 ($C_{ar.}$), 149.89 ($C_{ar.}$), 136.83 ($C_{ar.}$), 132.01 ($C_{ar.}$), 128.39 ($CH_{ar.}$), 125.70 ($CH_{ar.}$), 123.34 ($C_{ar.}$), 119.23 ($CH_{ar.}$), 115.59 ($CH_{ar.}$), 115.48 ($CH_{ar.}$), 40.04 (CH_3) ppm. IR (KBr disc): $\tilde{\nu}$ = 2999 (w), 2922 (m), 2870 (m), 2798 (w), 1627 (vs), 1571 (s), 1493 (m), 1456 (w), 1424 (w), 1396 (w), 1364 (s), 1264 (w), 1231 (m), 1136 (s), 1098 (w), 1061 (w), 1003 (w), 986 (m), 923 (w), 835 (w), 768 (w), 750 cm^{-1}. UV/Vis (CH_3CN, c = 1.03×10^{-5} mol L^{-1}): λ (ε, L mol^{-1} cm^{-1}) = 220 (8.37×10^4), 237 (8.39×10^4), 360 (3.87×10^4), 469 (3.4×10^3) nm. HRMS (ESI+): calcd. for $C_{20}H_{30}N_6$ [M + 2 H]$^{2+}$ 354.25265; found 354.25272; calcd. for $C_{40}H_{59}N_6$ [M + H]$^+$ 707.49802; found 707.49895.

4,4′,5,5′-Tetrakis(dimethylethyleneguanidinyl)binaphthyl (3b): To a solution of 1,3-dimethyl-2-imidazolidinone (1.0 mL, 9.3 mmol) dissolved in dry CHCl$_3$ (20 mL) was added oxalyl chloride (3.9 mL, 44.7 mmol) dropwise. The yellow solution was stirred at reflux for 20 h. The solvent was removed under vacuum. The remaining solid, 2-chloro-1,3-dimethylethyleneformamidinium chloride (9.3 mmol), was washed twice with Et$_2$O (8 mL), dissolved in dry CH$_2$Cl$_2$ (10 mL) and then added dropwise to a dry CH$_2$Cl$_2$ solution (25 mL) containing 4,4′,5,5′-tetraaminobinaphthyl (0.51 g, 1.64 mmol) and triethylamine (2.7 mL, 19.68 mmol) at –10 °C. The reaction mixture was stirred for an additional period of 3 h and warmed up slowly to room temperature during this time. The solution was extracted with HCl (5%) and then deprotonated with KOH solution (50%). After extracting with CH$_2$Cl$_2$, the combined organic phases were dried with K$_2$CO$_3$, and the solvent was removed under vacuum. The brown solid was extracted with hot toluene and filtered, and the toluene was removed under vacuum to afford the crude product. Upon recrystallization at –20 °C from an acetonitrile solution, 3b was obtained as a pale yellow-orange powder (0.417 g, 0.60 mmol, 37%). $C_{40}H_{50}N_{12}$ (698.91): calcd. C 68.74, H 7.21, N 24.05; found C 68.33, H 7.23, N 23.56. ^1H NMR (600.13 MHz, CD_2Cl_2): δ = 7.14 (d, J = 7.2 Hz, 2 H, CH$_{ar.}$), 6.93 (t, J = 7.8 Hz, 2 H, CH$_{ar.}$), 6.79 (d, J = 8.4 Hz, 2 H, CH$_{ar.}$), 6.66 (d, J = 7.2 Hz, 2 H, CH$_{ar.}$), 6.53 (d, J = 7.2 Hz, 2 H, CH$_{ar.}$), 3.25 (br. s, 16 H, CH$_2$), 2.65 [s, 12 H, N(CH$_3$)$_2$], 2.62 [br. s, 12 H, N(CH$_3$)$_2$] ppm. $^{13}C\{^1H\}$ NMR (159.99 MHz, CD_2Cl_2): δ = 151.13 (C=N), 150.95 (C=N), 149.19 ($C_{ar.}$), 148.30 ($C_{ar.}$), 136.44 ($C_{ar.}$), 132.30 ($C_{ar.}$), 128.06 ($CH_{ar.}$), 125.29 ($CH_{ar.}$), 124.57 ($C_{ar.}$), 119.53 ($CH_{ar.}$), 117.26 ($CH_{ar.}$), 117.15 ($CH_{ar.}$), 48.90 (CH_2), 35.09 (CH_3) ppm. IR (CsI disc): $\tilde{\nu}$ = 3032 (w), 2932 (m), 2845 (m), 1682 (s), 1577 (vs), 1487 (m), 1438 (w), 1390 (m), 1279 (m), 1242 (m), 1011 (m), 960 (m), 833 (w), 763 (w), 697 (w) cm^{-1}. MS (FAB): m/z (%) = 350.4 (42) [M + 2 H]$^{2+}$, 699.8 (100) [M + H]$^+$. UV/Vis (CH_3CN, c = 1.17×10^{-5} mol L^{-1}): λ (ε, L mol^{-1} cm^{-1}) = 219 (8.32×10^4), 237 (7.56×10^4), 358 (3.80×10^4) nm.

[(4a)H$_2$](PF$_6$)$_4$: To a solution of 3a dissolved in dry CH$_2$Cl$_2$ (20 mL) was added AgPF$_6$ (70.8 mg, 0.28 mmol). After stirring at room temperature in the dark for 24 h, the reaction mixture was filtered. The product was washed twice with dry CH$_2$Cl$_2$ (10 mL) and dried under vacuum (87%). Crystals of [(4a)H$_2$](PF$_6$)$_4$ suitable for XRD studies were grown by diffusion of CH$_2$Cl$_2$ into an acetonitrile solution at room temperature. ^1H NMR (399.89 MHz, CD$_3$CN): δ = 12.46 (s, 2 H, NH), 9.13 (d, ^3J = 9.8 Hz, 4 H, H$_{ar.}$), 7.35 (d, ^3J = 9.7 Hz, 4 H, H$_{ar.}$), 3.17 ppm [s, 48 H, N(CH$_3$)$_2$] ppm. ^{13}C NMR (150.92 MHz, CD$_3$CN): δ = 161.49 (C=N), 156.98, 135.69, 128.49, 126.42, 123.42, 112.29, 41.85 (CH$_3$) ppm. ^{31}P NMR (161.89 MHz, CD$_3$CN): δ = –144.62 (sept) ppm. IR (CsI disc): $\tilde{\nu}$ = 2942 (w), 1637 (m), 1529 (m), 1471 (w), 1408 (m), 1371 (w), 1294 (m), 1215 (w), 1172 (w), 1143 (w), 1064 (m), 1035 (w), 1008 (w), 839 (vs), 729 (m), 560 (s), 495 (m) cm^{-1}. UV/Vis (CH$_3$CN, c = 1.10×10^{-5} mol L^{-1}): λ (ε, L mol^{-1} cm^{-1}) = 212 (7.91×10^4), 232

(7.08×10^4), 288 (4.72×10^4), 374 (1.69×10^4), 462 (3.26×10^4), 487 (3.98×10^4), 554 (1.10×10^4) nm. Crystal data for $C_{40}H_{58}F_{24}N_{12}P_4$: M_r = 1286.86, $0.10 \times 0.08 \times 0.06$ mm, orthorhombic, space group $Pbam$, a = 14.715(14), b = 15.401(14), c = 12.396(10) Å, β = 90.00°, V = 2809(4) Å^3, Z = 2, $d_{calcd.}$ = 1.521 Mg m^{-3}, Mo-K_α radiation (graphite-monochromated, λ = 0.71073 Å), T = 100 K, θ_{range} = 1.91–25.02°. Reflections measd. 52111, indep. 2614, R_{int} = 0.1035. Final R indices [$I > 2\sigma(I)$]: R_1 = 0.0752, wR_2 = 0.1794.

[(4b)H$_2$](PF$_6$)$_4$: To a solution of 3b (47 mg, 0.067 mmol) dissolved in dry CH$_2$Cl$_2$ (20 mL) was added AgPF$_6$ (70.0 mg, 0.276 mmol). After stirring at room temperature in the dark for 24 h, the reaction mixture was filtered. The product was washed twice with dry CH$_2$Cl$_2$ (10 mL) and dried under vacuum (87%). $C_{40}H_{50}F_{24}N_{12}P_4$ (1278.28): calcd. C 37.57, H 3.94, N 13.14; found C 37.05, H 4.00, N 12.71. ^1H NMR (600.13 MHz, CD$_3$CN): δ = 12.65 (s, 2 H, NH), 9.18 (d, ^3J = 9.6 Hz, 4 H, H$_{ar.}$), 7.52 (d, ^3J = 9.6 Hz, 4 H, H$_{ar.}$), 4.09 (s, 8 H, CH$_2$) 3.97 (s, 8 H, CH$_2$), 2.99 [s, 24 H, N(CH$_3$)$_2$] ppm. ^{13}C NMR (150.90 MHz, CD$_3$CN): δ = 159.85 (C=N), 156.89, 135.64, 128.06, 125.98, 123.38, 111.10, 49.63 (CH$_2$), 34.11 (CH$_3$) ppm. MS (ESI+): m/z (%) = 232.7 (71.9) [M – 4 PF$_6$ – H]$^{3+}$, 348.4 (100) [M – 4 PF$_6$ – 2H]$^{2+}$. IR (CsI disc): $\tilde{\nu}$ = 2968 (w), 2929 (w), 1596 (s), 1553 (m), 1416 (w), 1356 (w), 1302 (m), 1211 (m), 1031 (w), 1012 (w), 974 (w), 835 (vs), 559 (s) cm^{-1}. UV/Vis (CH$_3$CN, c = 8.74×10^{-6} mol L^{-1}): λ (ε, L mol^{-1} cm^{-1}) = 216 (7.09×10^4), 287 (4.98×10^4), 375 (1.29×10^4), 460 (3.85×10^4), 486 (5.09×10^4), 599 (1.20×10^4) nm.

[(4a)H$_2$](I$_3$)$_3$I: To a solution of 3a (50.0 mg, 0.07 mmol) dissolved in dry CH$_3$CN (10 mL) was added dropwise a solution of iodine (88.8 mg, 0.35 mmol, 5 equiv.) dissolved in dry CH$_3$CN (10 mL). The reaction mixture was stirred at 50 °C for 1 h and at room temperature for an additional 4 d. After evaporation of the solvent, the remaining black solid was dried under vacuum at 110 °C to remove excessive iodine, washed with n-hexane and dried under vacuum to yield the product (57%). $C_{40}H_{58}I_{10}N_{12}$ (1976.02): calcd. C 24.31, H 2.96, N 8.51; found C 24.97, H 2.97, N 8.40. ^1H NMR (399.89 MHz, CD$_3$CN): δ = 12.48 (s, 2 H, NH), 9.22 (d, ^3J = 9.7 Hz, 4 H, H$_{ar.}$), 7.39 (d, ^3J = 9.6 Hz, 4 H, H$_{ar.}$), 3.21 [s, 48 H, N(CH$_3$)$_2$] ppm. MS (ESI+): m/z (%) = 176.7 (60.1) [M – 10 I]$^{4+}$, 235.5 (100.0) [M – 10 I – H]$^{3+}$, 352.3 (91.5) [M – 10 I – 2 H]$^{2+}$. IR (CsI disc): $\tilde{\nu}$ = 3020 (w), 2962 (w), 2930 (w), 2794 (w), 1616 (s), 1526 (vs), 1465 (m), 1438 (m), 1402 (s), 1290 (s), 1207 (m), 1171 (m), 1169 (m), 1061 (w), 1034 (w), 896 (w), 828 (w) cm^{-1}. UV/Vis (CH$_3$CN, c = 1.0×10^{-5} mol L^{-1}): λ (ε, L mol^{-1} cm^{-1}) = 208 (6.48×10^4), 291 (1.96×10^5), 364 (9.24×10^4), 463 (4.04×10^4), 488 (4.75×10^4), 552 (1.33×10^4), 596 (1.24×10^4) nm.

[(4b)H$_2$](I$_3$)$_3$I: To a solution of 3b (35.0 mg, 0.05 mmol) dissolved in dry CH$_3$CN (10 mL) was added dropwise a solution of iodine (68.0 mg, 0.268 mmol) dissolved in dry CH$_3$CN (10 mL). The reaction mixture was stirred at 50 °C for 1 h and at room temperature for an additional 4 d. After evaporation of the solvent, the remaining black solid was dried under vacuum at 110 °C to remove excess iodine, washed with n-hexane and dried under vacuum to yield the product (77%). $C_{40}H_{50}I_{10}N_{12}$ (1967.95): calcd. C 24.41, H 2.56, N 8.54; found C 24.48, H 2.62, N 8.35. ^1H NMR (200.13 MHz, CD$_3$CN): δ = 12.63 (s, 2 H, NH), 9.24 (d, ^3J = 9.6 Hz, 4 H, H$_{ar.}$), 7.56 (d, ^3J = 9.6 Hz, 4 H, H$_{ar.}$), 4.05 (br. s, 16 H, CH$_2$), 3.04 [s, 24 H, N(CH$_3$)$_2$] ppm. ^{13}C NMR (150.90 MHz, CD$_3$CN): δ = 159.91 (C=N), 156.83, 135.98, 128.32, 123.56, 111.49, 49.80 (CH$_2$), 34.74 (CH$_3$) ppm. MS (ESI+): m/z (%) = 174.9 (5.5) [M – 10 I]$^{4+}$, 232.7 (78.0) [M – 10 I – H]$^{3+}$, 348.3 (100.0) [M – 10 I – 2H]$^{2+}$, 696.4 (55.0) [M – 10 I – 2 H]$^+$. IR (CsI disc): $\tilde{\nu}$ = 3449 (m), 2967 (w), 2925 (w), 2875 (w), 1593 (vs), 1546 (s), 1435 (w), 1414 (w), 1370

(w), 1350 (m), 1298 (m), 1208 (m), 1030 (w), 1010 (w), 971 (w), 820 (w) cm^{-1}. UV/Vis (CH$_3$CN, c = 8.74 × 10^{-6} mol L^{-1}): λ (ε, L mol^{-1} cm^{-1}) = 210 (8.80 × 10^4), 292 (1.89 × 10^5), 362 (9.05 × 10^4), 487 (3.98 × 10^4) nm.

[κ^2-*N*,*N*′-3a(ZnCl$_2$)$_2$]: To a solution of **3a** (174.0 mg, 0.246 mmol) dissolved in acetonitrile (15 mL) was added dropwise a solution of ZnCl$_2$ in Et$_2$O (0.44 mL, 1 M, 0.44 mmol). The reaction mixture was stirred at room temperature for 24 h. After evaporation of the solvent, the residue was washed with toluene three times. The white product was dried in vacuo to yield 206.7 mg of product (0.211 mmol, 95%). Colourless crystals of [κ^2-*N*,*N*′-**3a**(ZnCl$_2$)$_2$]· 6CHCl$_3$ were obtained from a chloroform solution at –21 °C. C$_{40}$H$_{58}$Cl$_4$N$_{12}$Zn$_2$ (974.22): calcd. C 49.05, H 5.97, N 17.16; found C 48.90, H 6.10, N 16.86. ^{1}H NMR (600.13 MHz, CD$_2$Cl$_2$): δ = 7.27 (d, *J* = 7.58 Hz, 2 H, CH$_{ar.}$), 7.10 (dd, *J* = 7.91 Hz, 2 H, CH$_{ar.}$), 6.99 (d, *J* = 8.37 Hz, 2 H, CH$_{ar.}$), 6.44 (d, *J* = 7.59 Hz, 2 H, CH$_{ar.}$), 6.30 (d, *J* = 7.30 Hz, 2 H, CH$_{ar.}$), 2.95 (br. s, 48 H, CH$_3$) ppm. ^{13}C NMR (100.55 MHz, CD$_2$Cl$_2$): δ = 165.63 (CN$_3$), 165.56 (CN$_3$), 146.50 (C$_{ar.}$), 145.90 (C$_{ar.}$), 137.46 (C$_{ar.}$), 134.44 (C$_{ar.}$), 128.84 (CH$_{ar.}$), 126.36 (CH$_{ar.}$), 122.30 (CH$_{ar.}$), 121.71 (C$_{ar.}$), 118.14 (CH$_{ar.}$), 117.90 (CH$_{ar.}$), 41.55 (CH$_3$), 40.41 (CH$_3$) ppm. HRMS (ESI+): calcd. for C$_{40}$H$_{58}$N$_{12}$Cl$_3$Zn$_2$ [M – Cl]$^+$ 945.24763; found 945.24942. IR (KBr disc): $\tilde{\nu}$ = 3007 (w), 2939 (m), 2888 (m), 2794 (w), 1559 (vs), 1524 (vs), 1464 (m), 1400 (s), 1368 (m), 1331 (m), 1272 (w), 1236 (w), 1160 (s), 1105 (w), 1065 (w), 1019 (w), 1000 (m), 926 (w), 853 (w), 803 (w), 757 (w), 698 (w), 626 (w), 543 (w), 505 (w), 478 (w) cm^{-1}. Crystal data for C$_{46}$H$_{64}$Cl$_{22}$N$_{12}$Zn$_2$: M_r = 1697.77, 0.20 × 0.15 × 0.10 mm, monoclinic, space group *C*2/*c*, a = 29.187(6), b = 14.148(3), c = 17.919(4) Å, β = 96.52(3)°, V = 7352(3) Å^3, Z = 8, $d_{calcd.}$ = 1.532 Mg m^{-3}, Mo-K_α radiation (graphite-monochromated, λ = 0.71073 Å), T = 100 K, θ_{range} = 2.01–27.59°. Reflections measd. 16299, indep. 8431, R_{int} = 0.0224. Final R indices [I > 2σ(*I*)]: R_1 = 0.0553, wR_2 = 0.1613.

[(κ^2-*N*,*N*′-3b)(ZnCl$_2$)$_2$]: To a solution of **3b** (49.0 mg, 0.070 mmol) dissolved in acetonitrile (15 mL) was added dropwise a solution of ZnCl$_2$ (24 mg, 0.176 mmol) in acetonitrile (5 mL). During the addition an orange precipitate was formed. The reaction mixture was stirred at room temperature for 20 h. After partial removal of the solvent, the solution was filtered, and the orange precipitate was washed with cold acetonitrile (5 mL) and dried in vacuo. C$_{40}$H$_{50}$Cl$_4$N$_{12}$Zn$_2$ (971.54): calcd. C 49.45, H 5.19, N 17.30; found C 49.33, H 5.37, N 17.76. ^{1}H NMR (200.13 MHz, CD$_2$Cl$_2$): δ = 7.21 (d, *J* = 7.6 Hz, 2 H, CH$_{ar.}$), 7.07–6.91 (m, 4 H, CH$_{ar.}$), 6.68 (d, *J* = 7.6 Hz, 2 H, CH$_{ar.}$), 6.54 (d, *J* = 7.0 Hz, 2 H, CH$_{ar.}$), 3.64 (br. s, 16 H, CH$_2$), 2.94 (s, 6 H, CH$_3$), 2.93 (s, 6 H, CH$_3$), 2.89 (s, 6 H, CH$_3$), 2.84 (s, 6 H, CH$_3$) ppm. MS (ESI+): *m*/*z* (%) = 350.5 [M – 2 ZnCl$_2$ + 2 H]$^{2+}$, 699.5 (69.9) [M – 2 ZnCl$_2$ + H]$^+$, 764.8 (4.6) [M – ZnCl$_2$ – 2 Cl]$^+$, 834.9 (78.5) [M – ZnCl$_2$]$^+$. IR (CsI disc): $\tilde{\nu}$ = 3033 (w), 2933 (m), 2882 (m), 2802 (w), 1639 (m), 1563 (vs), 1480 (m), 1448 (m), 1412 (s), 1388 (s), 1297 (s), 1243 (m), 1013 (m), 971 (m), 840 (m), 812 (m), 760 (w), 700 (w), 633 (w) cm^{-1}.

[(4a)H$_2$][ZnI$_3$Cl]$_2$: To a solution of [κ^2-*N*,*N*′-(**3a**)(ZnCl$_2$)$_2$] (9.8 mg, 0.01 mmol) in acetonitrile (12 mL) was added an excess of I$_2$ (54 mg, 0.08 mmol) at room temperature. The reaction mixture was stirred at 50 °C for 2 h. NMR experiments indicated quantitative reaction to a single guanidine species. Dark green crystals of [(**4a**)H$_2$][ZnI$_3$Cl]$_2$·2CH$_3$CN suitable for XRD diffraction studies were obtained from this solution. However, this salt represents an intermediate; further reaction with I$_2$ leads finally to a product with the composition [(**4a**)H$_2$](I$_3$)$_3$I·2ZnCl$_2$. C$_{40}$H$_{58}$Cl$_4$I$_{10}$N$_{12}$Zn$_2$ (2248.59): calcd. C 21.4, H 2.6, N 7.5; found C 20.7, H 3.1, N 7.1. ^{1}H NMR (200.13 MHz, CD$_2$Cl$_2$): δ = 12.47 (s, 2 H, NH), 9.22 (d, 2 H, CH$_{ar.}$),

7.40 (d, 2 H, CH$_{ar.}$), 3.20 (s, 48 H, CH$_3$) ppm. Crystal data for C$_{44}$H$_{64}$Cl$_{3.3}$I$_{4.7}$N$_7$Zn$_2$: M_r = 1633.25, 0.20 × 0.15 × 0.15 mm, monoclinic, space group *P*2$_1$/*c*, a = 9.772(2), b = 14.753(3), c = 20.281(4) Å, β = 91.89(3)°, V = 2922.3(10) Å^3, Z = 2, $d_{calcd.}$ = 1.856 Mg m^{-3}, Mo-K_α radiation (graphite-monochromated, λ = 0.71073 Å), T = 100 K, θ_{range} = 2.50–27.56°. Reflections measd. 23324, indep. 6667, R_{int} = 0.0552. Final R indices [I > 2σ(*I*)]: R_1 = 0.0657, wR_2 = 0.1881.

4a: To a solution of [(**4a**)H$_2$](I$_3$)$_3$I (150 mg, 0.076 mmol) in acetonitrile was added hydrazine monohydrate (0.5 mL, 10.25 mmol) dropwise at room temperature. The ruby-coloured reaction mixture was stirred for 5 h. After removal of the solvent, the dark solid was dissolved in dichloromethane, and the insoluble residue was removed by filtration. After evaporation of the solvent, the dark product was dried under vacuum. ^{1}H NMR (399.89 MHz, CD$_3$CN): δ = 7.99 (d, 4 H, H$_{ar.}$), 6.65 (d, 4 H, H$_{ar.}$), 2.91 (s, 48 H, CH$_3$) ppm. ^{13}C NMR spectroscopic analysis was not possible owing to low solubility. MS (ESI+): *m*/*z* (%) = 705.4 (100.0) [MH]$^+$, 353.3 (62.2) [MH$_2$]$^{2+}$. UV/Vis (CH$_2$Cl$_2$): λ = 261, 355, 369, ca. 490, 525, 562 nm. Fluorescence spectroscopy (in CH$_2$Cl$_2$, excited at 520 nm): $\lambda_{e,max}$ = 586/625 nm.

4b: To a solution of [(**4b**)H$_2$](I$_3$)$_3$I (175 mg, 0.089 mmol) in acetonitrile was added hydrazine monohydrate (0.25 mL, 5.144 mmol) dropwise at room temperature. The reaction mixture immediately turned red and was stirred for 5 h. After removal of the solvent, the dark solid was dissolved in dichloromethane, and the insoluble residue was removed by filtration. The filtrate was concentrated, and the remaining product was dried under vacuum. ^{1}H NMR (200.13 MHz, CD$_3$CN): δ = 7.99 (d, *J* = 8.3 Hz, 4 H, H$_{ar.}$), 6.83 (d, *J* = 8.3 Hz, 4 H, H$_{ar.}$), 3.66 (br. s, 16 H, CH$_2$), 2.84 (br. s, 24 H, CH$_3$) ppm. ^{13}C NMR spectroscopic analysis was not possible owing to low solubility. MS (ESI+): *m*/*z* (%) = 348.4 (100) [M]$^{2+}$. UV/Vis (CH$_3$CN): λ = 214, 257, 356, ca. 487, 522, 549 nm. Fluorescence spectroscopy (in CH$_3$CN, excited at 514 nm): $\lambda_{e,max}$ = 623 nm.

X-ray Crystallographic Study: Suitable crystals were removed from the mother liquor, immersed in perfluorinated polyether oil and fixed on top of a glass capillary. Measurements were made with a Nonius-Kappa CCD diffractometer with a low-temperature unit using graphite-monochromated Mo-K_α radiation. The temperature was set to 100 K. The data collected were processed with the standard Nonius software.[24] All calculations were performed with the SHELXT-PLUS software package. Structures were solved by direct methods with the SHELXS-97 program and refined with the SHELXL-97 program.[25,26] Graphical handling of the structural data during solution and refinement was performed with XPMA.[27] Atomic coordinates and anisotropic thermal parameters of non-hydrogen atoms were refined by full-matrix least-squares calculations. In the case of [**4a**H$_2$](PF$_6$)$_4$, a full shell of intensity data was collected at low temperature (100 K) with a Bruker AXS Smart 1000 CCD diffractometer (Mo-K_α radiation, sealed tube, graphite monochromator). Data were corrected for air and detector absorption, Lorentz and polarization effects;[28] absorption by the crystal was treated with a semiempirical multiscan method.[29] The crystals were twinned; after detwinning (approx. twin fractions 0.73:0.27), structure solution and refinement were performed with all observations involving domain one. The structure was solved by the charge-flip procedure[30] and refined by full-matrix least-squares methods based on F^2 against all unique reflections. All non-hydrogen atoms were given anisotropic displacement parameters. Hydrogen atoms (except NH, which was refined) were input at calculated positions and refined with a riding model.[25] Owing

to severe disorder and fractional occupancy, electron density attributed to solvent of crystallization (acetonitrile) was removed from the structure (and the corresponding F_{obs}) with the BYPASS procedure,[31] as implemented in PLATON (SQUEEZE).[32] CCDC-891294 (for 4,4′-dinitrobinaphthyl), -891298 (for 4,4′,5,5′-tetranitrobinaphthyl), -891296 {for [κ²-*N*,*N*′-**3a**(ZnCl₂)₂]}, -891297 {for [(**4b**)H₂](PF₆)₄} and -891295 {for [(**4a**)H₂][ZnI₂.₃₅Cl₁.₆₅]₂} contain the supplementary crystallographic data for this paper. These data can be obtained free of charge from The Cambridge Crystallographic Data Centre via www.ccdc.cam.ac.uk/data_request/cif.

Supporting Information (see footnote on the first page of this article): UV/Vis spectra of **3b** and [(**4b**)H₂](PF₆)₄ in CH₃CN, CV curves for **3a** and **3b**, scheme with a possible explanation of the oxidation waves, IR spectra of [(**4a**)H₂](PF₆)₄, [(**4b**)H₂](PF₆)₄, [(**4a**)H₂](I₃)₃I and [(**4a**)H₂](I₃)₃I, UV/Vis and emission spectrum of **4b**, and structure of the tetracation in [(**4a**)H₂][ZnI₃Cl]₂.

[1] a) F. T. Edelmann, *Adv. Organomet. Chem.* **2008**, *57*, 183–352; b) F. T. Edelmann, *Coord. Chem. Rev.* **1994**, *137*, 403–481.

[2] a) J. Barker, M. Kilner, *Coord. Chem. Rev.* **1994**, *133*, 219–300; b) P. J. Bailey, S. Price, *Coord. Chem. Rev.* **2001**, *214*, 91–141.

[3] S. Herres-Pawlis, *Nachr. Chem.* **2009**, *57*, 20–23.

[4] a) M. P. Coles, *Dalton Trans.* **2006**, 985–1001; b) M. P. Coles, *Chem. Commun.* **2009**, 3659–3676.

[5] C. Jones, *Coord. Chem. Rev.* **2010**, *254*, 1273–1289.

[6] H.-J. Himmel in *Modeling of Molecular Properties* (Ed.: P. Comba), Wiley-VCH, Weinheim, **2011**.

[7] a) J. Börner, U. Flörke, K. Huber, A. Döring, D. Kuckling, S. Herres-Pawlis, *Chem. Eur. J.* **2009**, *15*, 2362–2376; b) J. Börner, I. dos Santos Vieira, A. Pawlis, A. Doering, D. Kuckling, S. Herres-Pawlis, *Chem. Eur. J.* **2011**, *17*, 4507–4512; c) J. Börner, I. dos Santos Vieira, M. D. Jones, A. Doering, D. Kuckling, U. Flörke, S. Herres-Pawlis, *Eur. J. Inorg. Chem.* **2011**, 4441–4456; d) I. dos Santos Vieira, S. Herres-Pawlis, *Eur. J. Inorg. Chem.* **2012**, 765–774; e) I. dos Santos Vieira, S. Herres-Pawlis, *Z. Naturforsch. B* **2012**, *67*, 320–330.

[8] a) M. Schatz, V. Raab, S. P. Foxon, G. Brehm, S. Schneider, M. Reiher, M. C. Holthausen, J. Sundermeyer, S. Schindler, *Angew. Chem.* **2004**, *116*, 4460–4464; *Angew. Chem. Int. Ed.* **2004**, *43*, 4360–4363; b) C. Würtele, E. Gaoutchenova, K. Harms, M. C. Holthausen, J. Sundermeyer, S. Schindler, *Angew. Chem.* **2006**, *118*, 3951–3954; *Angew. Chem. Int. Ed.* **2006**, *45*, 3867–3869; c) D. Maiti, D.-H. Lee, K. Gaoutchenova, C. Würtele, M. C. Holthausen, A. A. Narducci Sarjeant, J. Sundermeyer, S. Schindler, K. D. Karlin, *Angew. Chem.* **2007**, *120*, 88–91; *Angew. Chem. Int. Ed.* **2007**, *47*, 82–85; d) D. Maiti, D.-H. Lee, A. A. Narducci Sarjeant, M. Y. M. Pau, E. I. Solomon, K. Gaoutchenova, J. Sundermeyer, K. D. Karlin, *J. Am. Chem. Soc.* **2008**, *130*, 6700–6701; e) J. S. Woertink, L. Tian, D. Maiti, H. R. Lucas, R. A. Himes, K. D. Karlin, F. Neese, C. Würtele, M. C. Holthausen, E. Bill, J. Sundermeyer, S. Schindler, E. I. Solomon, *Inorg. Chem.* **2010**, *49*, 9450–9459.

[9] A. Neuba, R. Haase, W. Meyer-Klaucke, U. Flörke, G. Henkel, *Angew. Chem.* **2012**, *124*, 1746–1750; *Angew. Chem. Int. Ed.* **2012**, *51*, 1714–1718.

[10] P. Roquette, A. Maronna, A. Peters, E. Kaifer, H.-J. Himmel, Ch. Hauf, V. Herz, E.-W. Scheidt, W. Scherer, *Chem. Eur. J.* **2010**, *16*, 1336–1350.

[11] A. Peters, E. Kaifer, H.-J. Himmel, *Eur. J. Org. Chem.* **2008**, 5907–5914.

[12] V. Vitske, C. König, E. Kaifer, O. Hübner, H.-J. Himmel, *Eur. J. Inorg. Chem.* **2010**, 115–126.

[13] D. Emeljanenko, A. Peters, V. Vitske, E. Kaifer, H.-J. Himmel, *Eur. J. Inorg. Chem.* **2010**, 4783–4789.

[14] A. Peters, H. Herrmann, M. Magg, E. Kaifer, H.-J. Himmel, *Eur. J. Inorg. Chem.* **2012**, 1620–1631.

[15] a) A. Peters, C. Trumm, M. Reinmuth, D. Emeljanenko, E. Kaifer, H.-J. Himmel, *Eur. J. Inorg. Chem.* **2009**, 3791–3800; b) D. Emeljanenko, A. Peters, N. Wagner, J. Beck, E. Kaifer, H.-J. Himmel, *Eur. J. Inorg. Chem.* **2010**, 1839–1846; c) C. Trumm, E. Kaifer, O. Hübner, H.-J. Himmel, *Eur. J. Inorg. Chem.* **2010**, 3102–3108.

[16] a) M. Reinmuth, U. Wild, E. Kaifer, M. Enders, H. Wadepohl, H.-J. Himmel, *Eur. J. Inorg. Chem.* **2009**, 4795–4808; b) P. Roquette, C. König, O. Hübner, N. Wagner, E. Kaifer, M. Enders, H.-J. Himmel, *Eur. J. Inorg. Chem.* **2010**, 4770–4782; c) D. Emeljanenko, E. Kaifer, H. Wadepohl, H.-J. Himmel, *Eur. J. Inorg. Chem.* **2012**, 695–704; d) C. Trumm, S. Stang, B. Eberle, E. Kaifer, N. Wagner, J. Beck, T. Bredow, O. Hübner, H.-J. Himmel, *Eur. J. Inorg. Chem.* **2012**, 3156–3167.

[17] V. Vitske, P. Roquette, S. Leingang, C. Adam, E. Kaifer, H. Wadepohl, H.-J. Himmel, *Eur. J. Inorg. Chem.* **2011**, 1593–1604.

[18] V. Raab, J. Kipke, R. M. Gschwind, J. Sundermeyer, *Chem. Eur. J.* **2002**, *8*, 1682–1693.

[19] U. Wild, O. Hübner, A. Maronna, M. Enders, E. Kaifer, H. Wadepohl, H.-J. Himmel, *Eur. J. Inorg. Chem.* **2008**, 4440–4447.

[20] L. A. Jones, C. T. Joyner, *J. Chem. Eng. Data* **1973**, *18*, 105–108.

[21] a) R. A. Friedel, M. Orchin, L. Reggel, *J. Am. Chem. Soc.* **1948**, *70*, 199–204; b) J. C. Del Riccio, F. Zhang, A. R. Lacey, S. H. Kable, *J. Phys. Chem. A* **2000**, *104*, 7442–7451.

[22] A. Maronna, E. Bindewald, E. Kaifer, H. Wadepohl, H.-J. Himmel, *Eur. J. Inorg. Chem.* **2011**, 1302–1314.

[23] See, for example: L. Feiler, H. Langhals, K. Polborn, *Liebigs Ann.* **1995**, 1229–1244.

[24] DENZO-SMN, Data processing software, Nonius **1998**; http://www.nonius.nl.

[25] a) G. M. Sheldrick, *SHELXS-97, Program for Crystal Structure Solution*, University of Göttingen, **1997**; http://shelx.uni-ac.gwdg.de/SHELX/index.html; b) G. M. Sheldrick, *SHELXL-97, Program for Crystal Structure Refinement*, University of Göttingen, **1997**; http:// shelx.uni-ac.gwdg.de/SHELX/index.html; c) G. M. Sheldrick, *Acta Crystallogr., Sect. A* **2008**, *64*, 112.

[26] *International Tables for X-ray Crystallography*, vol. 4, Kynoch Press, Birmingham, U. K., **1974**.

[27] L. Zsolnai, G. Huttner, XPMA, University of Heidelberg, **1994**; http://www.uni-heidelberg.de/institute/fak12/AC/huttner/software/software.html.

[28] *SAINT*, Bruker AXS, Karlsruhe **1997–2008**.

[29] R. H. Blessing, *Acta Crystallogr., Sect. A* **1995**, *51*, 33; G. M. Sheldrick, *TWINABS*, Bruker AXS, Karlsruhe **2004–2008**.

[30] a) L. Palatinus, *SUPERFLIP*, EPF Lausanne, Switzerland, **2007**; b) L. Palatinus, G. Chapuis, *J. Appl. Crystallogr.* **2007**, *40*, 786.

[31] P. v. d. Sluis, A. L. Spek, *Acta Crystallogr., Sect. A* **1990**, *46*, 194.

[32] a) A. L. Spek, *PLATON*, Utrecht University, The Netherlands; b) A. L. Spek, *J. Appl. Crystallogr.* **2003**, *36*, 7.